

Effects of TAT-conjugated platinum nanoparticles on lifespan of mitochondrial electron transport complex I-deficient *Caenorhabditis elegans*, *nuo-1*

Yuri Sakaue
Juewon Kim
Yusei Miyamoto

Department of Integrated
Biosciences, University of Tokyo,
Chiba, Japan

Abstract: Platinum nanoparticle (Pt-np) species are superoxide dismutase/catalase mimetics and also have an activity similar to that of mitochondrial electron transport complex I. To examine if this complex I-like activity functions *in vivo*, we studied the effects of Pt-nps on the lifespan of a mitochondrial complex I-deficient *Caenorhabditis elegans* mutant, *nuo-1* (LB25) compared with wild-type N2. We synthesized a fusion protein of a cell-penetrating peptide, human immunodeficiency virus-1 TAT (48–60), C-terminally linked to a peptide with a high affinity to platinum (GRKKRRQRRRPPQ-DRTSTWR). Pt-nps were functionalized by conjugation with this fusion protein at a 1:1 ratio of TAT-PtBP to Pt atoms. Adult worms were treated with conjugated Pt-nps for 10 days. The mean lifespan of untreated N2 and LB25 was 19.6 ± 0.4 and 11.8 ± 0.3 days, respectively. Using $5 \mu\text{M}$ of conjugated Pt-nps, the lifespan of N2 and LB25 was maximally extended. This maximal lifespan extension of LB25 was $31.9 \pm 2.6\%$, which was significantly greater than that of N2 ($21.1 \pm 1.7\%$, $P < 0.05$ by Student's *t*-test). Internalization of Pt into the whole body and mitochondria was similar between these two strains. Excessive accumulation of reactive oxygen species was not observed in the cytosol or mitochondria of untreated LB25. Treatment for five days with $5 \mu\text{M}$ conjugated Pt-nps decreased cytosolic and mitochondrial reactive oxygen species in N2 and LB25 to a similar extent. The ratio of $[\text{NAD}^+]/[\text{NADH}]$ was very low in the whole body and mitochondria of control LB25. After five days of treatment with $5 \mu\text{M}$ conjugated Pt-nps, the ratio of $[\text{NAD}^+]/[\text{NADH}]$ was increased in N2 and LB25. However, the degree of the increase was much higher in LB25 than in N2. Pt-nps function as NADH oxidase and recover the $[\text{NAD}^+]/[\text{NADH}]$ ratio in LB25, leading to effective extension of the lifespan of LB25.

Keywords: platinum nanoparticles, *Caenorhabditis elegans*, complex I-deficient mutant, LB25, lifespan

Introduction

Platinum nanoparticles (Pt-nps) are an efficient catalyst for electro-oxidation of hydrogen peroxide (H_2O_2).¹ Owing to this catalase activity, Pt-nps are utilized as a fine element of biosensors.^{2,3} However, Pt-nps have not been developed sufficient for biologic or medical use compared with gold nanoparticles (Au-nps).^{4–6} Recently, some papers have shown biologic and medical application of Pt-nps, including usage as a platform for drug delivery.^{7–9} We regard Pt-nps as a bioactive material, ie, a kind of antioxidant, and have undertaken research on these entities. *In vitro* Pt-nps scavenge reactive oxygen species (ROS) including superoxide anion (O_2^-) as well as H_2O_2 , and free radicals.^{1,10} Pt-nps seem to have catalytic antioxidant activity. Because the O_2^- -scavenging activity of Au-nps is less than that of

Correspondence: Yusei Miyamoto
Department of Integrated Biosciences,
Graduate School of Frontier Sciences,
University of Tokyo, Bioscience Building
402, 5-1-5 Kashiwanoha, Kashiwa, Chiba
277–8562, Japan
Tel +81 471 36 3628
Fax +81 471 36 3630
Email yusei74@k.u-tokyo.ac.jp

Pt-nps, and Au-nps cannot scavenge H_2O_2 , Pt-nps are a more potent antioxidant than Au-nps.¹ *In vivo* we tested the effects of Pt-nps on the lifespan of *Caenorhabditis elegans*.¹¹ Pt-nps extended the lifespan of wild-type N2 and the mitochondrial electron transport complex II mutant, *mev-1(kn1)*, whereas a well known superoxide dismutase/catalase mimetic, EUK-8, did not do this. Furthermore, Pt-nps exhibited more effective protection of nematodes against acute oxidative stress induced by paraquat than EUK-8. These data suggest that Pt-nps scavenge excessive oxidative stress to elongate the lifespan and survival of nematodes.

Mitochondrial electron transport complex I consists of many subunits and is located in the mitochondrial inner membrane.¹² This complex is NADH:ubiquinone oxidoreductase that transfers electrons from NADH in the matrix to ubiquinone in the inner membrane, with proton transport from the matrix to the mitochondrial intramembrane space. In some diseases the complex I is deficient or its enzymatic activity is suppressed, leading to generation of an excessive amount of O_2^- . Accumulated ROS seem to contribute partially to the pathogenesis of those diseases.^{13–16} Recently, we have shown *in vitro* that Pt-nps have an activity similar to the complex I that drives oxidation of NADH to NAD^+ , as well as reduction of ubiquinone to ubiquinol.¹⁷ Although it is still not known if Pt-nps transport protons, we expect that Pt-np species will be an enzymatic mimetic of mitochondrial complex I. Pt-nps are able to mediate oxidation of NADH and reduction of ubiquinone separately. In other words, Pt-nps do not require electrons from NADH to reduce ubiquinone. We suspect that Pt-nps may accept and release electrons by interaction with water molecules.

A mitochondrial complex I-deficient *C. elegans* mutant, LB25, is a transgenic strain expressing the *nuo-1* (NADH:ubiquinone oxidoreductase) gene carrying an A352V mutation.¹⁸ The *nuo-1* gene is the *C. elegans* homolog of the human *NDUFV1* (NADH dehydrogenase ubiquinone flavoprotein 1) gene encoding the active site subunit of complex I. The A352V mutation corresponds to the residue A341 of the human *NDUFV1* gene which causes severe neurologic disorders and muscle atrophy in early childhood.¹³ In this study, we describe the significance of Pt-nps as a mitochondrial complex I mimetic, as well as an antioxidant, in partial recovery of the short lifespan of LB25, indicating that Pt-np species may be a new potent material for diseases with dysfunctional mitochondrial complex I.

Material and methods

C. elegans and growth conditions

Wild-type N2 and a mitochondrial complex I-deficient mutant *C. elegans*, *nuo-1* (LB25), were obtained from the *Caenorhabditis* Genetic Center (University of Minnesota, St Paul, MN). These strains were maintained at 20°C by a popular procedure established by Brenner.¹⁹ Age-synchronous populations were prepared as previously described.¹¹ Briefly, collected eggs were allowed to hatch overnight at 20°C in 1 mL of S-basal buffer (100 mM NaCl, 0.01 mM cholesterol, and 50 mM potassium phosphate, pH 6.0), on nematode growth medium agar plates.²⁰ Hatched worms (L1 larval stage) were transferred to fresh nematode growth medium agar plates with *Escherichia coli* OP50 as a food source, and cultured at 20°C until the L4 larval stage.

Preparation of Pt-nps

Pt-nps were prepared by an ethanol reduction method of hydrogen hexachloroplatinate (H_2PtCl_6) using poly(N-vinyl-2-pyrrolidone, PVP) as a protecting reagent.¹¹ PVP, $H_2PtCl_6 \cdot 6H_2O$, and ethanol were purchased from Wako Pure Chemical Industries (Osaka, Japan). Water was freshly prepared with a Millipore Milli-Q Academic Water Purification System (Millipore, Billerica, MA). We estimated the concentration of Pt in Pt-nps from the concentration of $PtCl_6^{2-}$ in a starting reaction mixture, assuming 100% reduction of Pt^{4+} to Pt. Therefore, the Pt-nps concentrations reported herein actually refer to the estimated concentration of Pt atoms present in Pt-nps.

The human immunodeficiency virus (HIV)-1 protein, TAT, is a transcriptional activator of HIV. TAT consists of 86 amino acids, but its translocation activity is associated with the peptide sequence (48–60; GRKKRRQRRRPPQ).²¹ A short peptide (DRTSTWR) is known to be one with high affinity to platinum and is referred to here as a platinum-binding peptide (PtBP).²² A fusion peptide was synthesized by C-terminally linking of HIV-1 TAT (48–60) to PtBP (GRKKRRQRRRPPQ-DRTSTWR). Pt-nps protected with PVP (PVP-Pt) were conjugated with this fusion protein (TAT-PtBP) at a 1:1 ratio of TAT-PtBP to Pt atom to increase the internalization of Pt-nps into worms.²³ The consequent conjugate was designated as TAT-PtBP-Pt. Therefore, unconjugated Pt-nps indicates PVP-Pt.

Lifespan assay

For the lifespan assay, synchronous L4 larvae were transferred to S-medium (S-basal medium supplemented with 3 mM $CaCl_2$, 3 mM $MgSO_4$, 50 μ M ethylenediamine tetraacetic

acid [EDTA], 25 μM FeSO_4 , 10 μM MnCl_2 , 10 μM ZnSO_4 , 1 μM CuSO_4 , and 10 mM KH_2PO_4 , at pH 6.0) with *E. coli* OP50.²⁴ We chose a liquid medium because it was difficult to make an agar plate in which TAT-PtBP-Pt were evenly distributed and, furthermore, because worms were allowed to make contact freely with TAT-PtBP-Pt. This transfer day was recorded as Day 0. Nematodes were treated with TAT-PtBP-Pt for 10 days from Day 0. The worms were transferred to fresh culture medium every second day, and the surviving worms were counted at the same time. Worms that died unnaturally were excluded. The mortality data were subjected to Kaplan–Meier survival analysis to prepare survival curves. Statistical comparisons of mean lifespan values between untreated (control) and treated worms were analyzed by Peto's log-rank test.

Isolation of mitochondria

Isolation of mitochondria was performed as previously described.¹⁸ Worms were collected from liquid culture and rinsed three times with M9 buffer (3 g/L KH_2PO_4 , 6 g/L Na_2HPO_4 , and 5 g/L NaCl supplemented with 1 mM MgSO_4 and 0.02% gelatin after autoclaving). Rinsed worms were suspended in 0.2 M mannitol, 70 mM sucrose, 0.1 M EDTA, and 1 mM phenylmethylsulfonyl fluoride at pH 7.4. Worms were homogenized 10 times by a BRANSON Sonifier 150 with a 3 mm diameter probe (Branson Ultrasonic Co., Danbury, CT). Homogenized samples were centrifuged three times at $1000 \times g$ for 10 minutes to eliminate unbroken cells and cuticles. The supernatant was then centrifuged at $19,200 \times g$ for 10 minutes to precipitate mitochondria. The pellet was suspended in 0.2 M mannitol, 70 mM sucrose, and 0.1 M EDTA, pH 7.4 (MSE buffer) and centrifuged again. The resultant sediment containing mitochondria was resuspended in 0.5 mL MSE buffer. Protein concentration was estimated by the Bradford method with a commercially available kit (Bio-Rad, Hercules, CA).

Measurement of platinum content

On Day 0, treatments of N2 and LB25 with 5 μM TAT-PtBP-Pt were started and continued for five days. Nematodes treated with unconjugated PVP-Pt served as controls. Treated nematodes were rinsed three times with M9 buffer and transferred to crucibles with 1 mL of 1% nitric acid, 60% perchloric acid, and 35% chloric acid.²³ The samples were heated and volatilized at 200°C using an electric hot plate, followed by heating with 1 mL of 1% nitric acid three times. Finally, the samples were resuspended in 5 mL of 1% nitric acid. Determination of amount of Pt in the resuspended samples was performed.

Measurements of Pt internalized in mitochondria were performed using similar procedures. The statistical significance of differences between the control and treated groups was determined by Student's *t*-test.

Measurement of reactive oxygen species

N2 and LB25 nematodes were treated with 5 μM TAT-PtBP-Pt for five days from Day 0. On day 5, the treated nematodes were washed three times with M9 buffer. The worms were then incubated for 30 minutes at 20°C in 2 mL of Hank's solution (0.44 mM KH_2PO_4 , 5.37 mM KCl, 0.34 mM Na_2HPO_4 , 136.89 mM NaCl, and 5.55 mM D-glucose) containing 10 μM 5-(and 6)-chloromethyl-2',7'-dichlorodihydrofluorescein diacetate acetyl ester (CM-H₂DCFDA) (Sigma-Aldrich Co., St. Louis, MO) and/or MitoSOX™ Red (MitoSox, obtained from Invitrogen, Carlsbad, CA).¹¹ CM-H₂DCF released by esterase and MitoSox were fluorescent dyes to assay cytosolic ROS mainly consisting of H_2O_2 and mitochondrial O_2^- , respectively. Worms were fixed with 4% formaldehyde and mounted on 2% agarose pads. To determine the fluorescence of CM-H₂DCF and MitoSOX, fixed nematode samples were subjected to Leica TCS SP2 laser scanning confocal microscopy (CM-H₂DCF, excitation at 488 nm and emission at 510 nm; MitoSOX, excitation at 510 nm and emission at 580 nm). The relative fluorescence of the whole body was determined densitometrically using the LCS Lite software. The statistical significance of differences between the control and treated groups was determined by Student's *t*-test.

NAD⁺ and NADH assays

Nematodes were treated with 5 μM TAT-PtBP-Pt for five days from Day 0. On Day 5, treated animals were rinsed three times with M9 buffer. Rinsed worms were suspended in 100 mM NaCl, 1% NP-40, 1 mM DTT, 10% glycerol, and 100 mM Tris, at pH 8. Worms were homogenized 10 times by BRANSON Sonifier 150 with a 3 mm diameter probe. Protein concentration was estimated by the Bradford method. We used an NAD⁺/NADH assay kit (Gentaur, Kampenhout, Belgium). Homogenized samples were mixed with 100 μL of NAD⁺ extraction buffer for NAD⁺ estimation or NADH extraction buffer for NADH estimation and heated at 60°C for five minutes. Twenty microliters of assay buffer and 100 μL of NADH (or NAD⁺) extraction buffer were added. Samples were then vortexed and spun at $10,000 \times \text{rpm}$ for five minutes. The resultant supernatant was used for NAD⁺ and NADH assays. Similar procedures were performed to determine NAD⁺ and NADH in isolated mitochondria. The statistical

significance of differences between the control and treated groups was determined by Student's *t*-test.

Results and discussion

TAT-PtBP-Pt extends lifespan of wild-type N2 and *nuo-1* mutant

The survival of control wild-type N2 and mutant LB25 delineates regular reverse-sigmoid curves (Figure 1A). The mutants died earlier than the wild type. Treatment with 5 μ M TAT-PtBP-Pt for 10 days from Day 0 shifts the survival curves of N2 and LB25 to the right, indicating extension of their lifespan. The mean lifespan was obtained by calculating the data of the survival curves. The mean lifespans of control N2 and LB25 were 19.6 ± 0.4 and 11.8 ± 0.3 days, respectively, indicating that the mean lifespan of LB25 is approximately 40% less than that of N2 (see Table). This result is in good accordance with a previous report.¹⁸ The concentration of TAT-PtBP-Pt was varied from 1–25 μ M. While the lifespan of N2 was significantly extended by TAT-

PtBP-Pt only at 5 μ M ($***P < 0.001$), the mutant lifespan was extended by more than 5 μ M and was maximal at 5 μ M ($**P < 0.01$ (10 and 25 μ M), $***P < 0.001$ (5 μ M), as shown in Figure 1B and Table 1). The maximal lifespan of LB25 was 15.6 ± 0.4 days by $31.9 \pm 2.6\%$ increase of their control lifespan (see Table 1). Treatment of N2 with 5 μ M TAT-PtBP-Pt extended the mean lifespan to 23.3 ± 0.4 days only by $21.1 \pm 1.7\%$. TAT-PtBP at 25 μ M alone did not affect either N2 or LB25 lifespan (Figure 1B and Table 1). These data suggest that Pt in TAT-PtBP-Pt is the active source of the nematode lifespan extension, and the lifespan extension by Pt-nps is significantly more effective in LB25 than in N2 ($P < 0.05$ by Student's *t*-test).

Recently, we have performed a similar experiment to monitor the lifespan extension of wild-type nematode N2 by conjugation of Pt-nps with TAT-PTBP.²³ The lifespan of control N2 was 18.0 ± 0.3 days. Treatment with TAT-PtBP-Pt significantly elongated the lifespan in the concentration range 1–50 μ M ($P < 0.001$). The maximal extension of lifespan

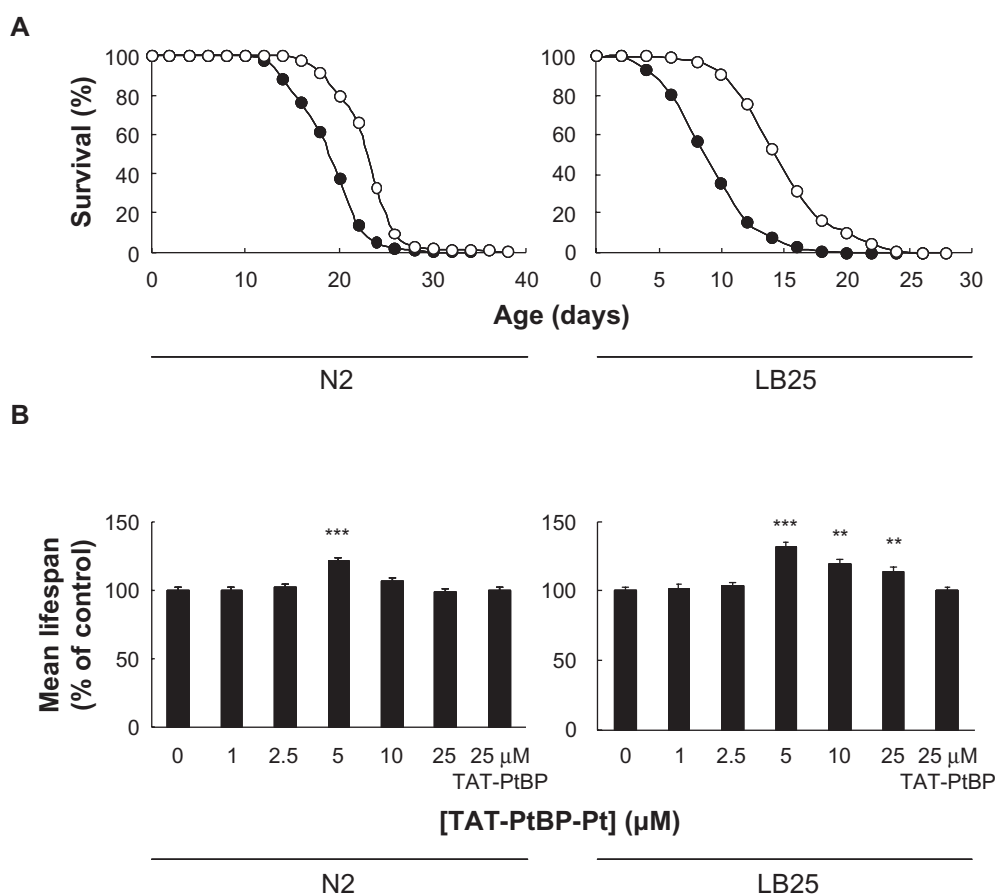


Figure 1 Effects of TAT-PtBP-Pt on the lifespan of N2 and LB25. Adult nematodes were treated with 5 μ M TAT-PtBP-Pt for days 0–10. Shown are survival curves of untreated control (●) and treated (○) worms **A**). The number of worms was 90–95 in each experiment, and three independent experiments were repeated. The mean lifespan **B**) was calculated from survival curves. The concentration of Pt in TAT-PtBP-Pt was varied up to 25 μ M. Effect of the fusion protein (TAT-PtBP) at 25 μ M alone on the lifespan of nematodes was also studied. Error bars represent the standard error of the mean.

Notes: $**P < 0.01$; $***P < 0.001$, as compared with control worms by the log-rank test. The lifespan data are summarized in the Table.

Table 1 Effects of TAT-PtBP-Pt on the lifespan of *C. elegans*

Strain	Treatment	μM	MLS	%	P	n	
N2	Control	0	19.6 ± 0.4			91	
	TAT-PtBP-Pt	1	19.5 ± 0.4	-0.2 ± 2.0	0.628	90	
		2.5	19.9 ± 0.4	1.9 ± 1.7	0.447	90	
		5	23.3 ± 0.4	21.1 ± 2.0	3.04E-7	90	
		10	20.9 ± 0.4	6.8 ± 1.9	0.171	90	
		25	19.3 ± 0.4	-1.5 ± 2.1	0.462	90	
	TAT-PfBP	25	19.3 ± 0.4	0 ± 2.1	0.575	90	
	LB25	Control	0	11.8 ± 0.3			93
		TAT-PtBP-Pt	1	12.0 ± 0.3	2.0 ± 2.5	0.754	90
			2.5	12.2 ± 0.3	3.4 ± 2.5	0.684	90
5			15.6 ± 0.4	31.9 ± 2.6	2.73E-4	95	
10			14.0 ± 0.3	18.9 ± 3.6	1.39E-3	95	
25			13.5 ± 0.4	14.1 ± 3.0	9.36E-3	95	
TAT-PtBP		25	11.9 ± 0.3	0.6 ± 2.5	0.887	90	

Notes: MLS, mean lifespan (days) presented as mean \pm SEM; %, change in MLS compared with control, presented as mean \pm SEM.

Abbreviations: SEM, standard error of the mean; MLS, mean lifespan; n, number of deaths observed.

was observed with 5 μM TAT-PtBP-Pt. The maximal mean lifespan was 22.4 \pm 0.4 days, resulting in an increase of 24%. The experimental difference between our previous and current studies is the treatment period. Nematodes were treated until death in the previous study, but only for 10 days in the current study.

The optimal increase of life span by TAT-PtBP-Pt was observed at 5 μM . Greater concentrations of TAT-PtBP-Pt showed less positive effects. Currently, we do not have a clear explanation for this phenomenon. A possible speculation is that the lifespan extension by Pt-nps may gradually decrease with the concentration increase due to toxicity. Pt-nps may extend lifespan by activating cellular signaling via a small change of ROS, but not by a big change.²⁵ Further studies are required.

Similar internalization of Pt-nps by N2 and *nuo-1*

The amount of Pt internalized in N2 and LB25 whole bodies by treatment with 5 μM unconjugated PVP-Pt for five days from Day 0 was 3.30 \pm 0.05 and 3.33 \pm 0.12 ng/worm, respectively (Figure 2A). Conjugation of Pt-nps with TAT-PtBP enhances Pt internalization approximately six times in both nematodes ($***P < 0.001$; amount of internalized Pt in N2 and LB25 whole bodies, 19.9 \pm 0.4 and 21.3 \pm 0.9 ng/worm, respectively). The mitochondrial Pt accumulation from PVP-Pt was approximately 1% of the whole body Pt accumulation (29.1 \pm 0.8 and 22.7 \pm 0.3 pg/worm in N2 and LB25 mitochondria, respectively, Figure 2B). Although TAT was used as a

cell-penetrating peptide (CPP), it was significantly effective even in mitochondrial translocation ($***P < 0.001$; N2 and LB25, 55.3 \pm 2.0 and 55.7 \pm 0.3 ng/worm, respectively). There was not a significant difference in whole body or mitochondrial accumulation of Pt from TAT-PtBP-Pt between these two strains. Therefore, the more effective lifespan extension of LB25 than N2 by treatment with 5 μM TAT-PtBP-Pt is not due to the higher permeability of Pt in LB25 than N2.

CPPs are referred to as protein transduction domains and utilized to facilitate cellular uptake of hydrophilic bioactive large molecules.²⁶ TAT is one of the popular CPPs and successful in delivery of proteins, peptides, and nucleotides across the cell membrane.²⁷ TAT has been used for protein delivery, even in *C. elegans*.²⁸ CPPs are usually linked to cargoes by covalent binding.²⁹ For example, in the case of Au-nps, tiopronin, a kind of spacer, was first covalently bound to gold atoms via a sulfhydryl group during reduction of AuCl_4^- by NaBH_4 .³⁰ TAT was then covalently bound to tiopronin to functionalize the Au-nps. We used PtBP to link TAT to Pt-nps.²³ This is a unique approach to transcellular delivery of metal-nps. Although precise mechanisms for internalization of Pt-nps into nematodes are unknown, we assume that intestinal permeability of Pt-nps is enhanced by conjugation with TAT-PtBP. Previous studies have shown that TAT conjugation leads Au-nps to nuclear translocation in cells.^{30,31} Furthermore, CPPs interrupt mitochondrial targeting.³² Our results indicate that TAT-PtBP conjugation facilitates mitochondrial translocation of Pt-nps to a small but significant extent. We need more sophisticated research on intracellular localization of TAT conjugated Pt-nps.

Reactive oxygen species in cytosol and mitochondria of N2 and *nuo-1*

The effects of TAT-PtBP-Pt treatment on ROS were investigated in N2 and LB25. Typical fluorescence from cytosolic CM- H_2DCF in the whole body is shown in Figure 3A–D (A, control N2; B, treated N2; C, control LB25; D, treated LB25). The fluorescent intensity obtained using LCS Lite software was similar between control N2 and LB25 (46.4 \pm 2.8 and 42.5 \pm 2.8, respectively). The relative fluorescence is shown in Figure 3E. Treatment with 5 μM TAT-PtBP-Pt for five days from Day 0 significantly decreased the fluorescence, and the extent of this reduction was also similar between these two strains (-39.2 \pm 2.1 and -33.7 \pm 1.8%, respectively, $*P < 0.05$). Mitochondrial O_2^- was also measured with MitoSox in Figure 4A–D; A, control N2; B, treated N2; C, control LB25; D, treated LB25). The fluorescent intensity

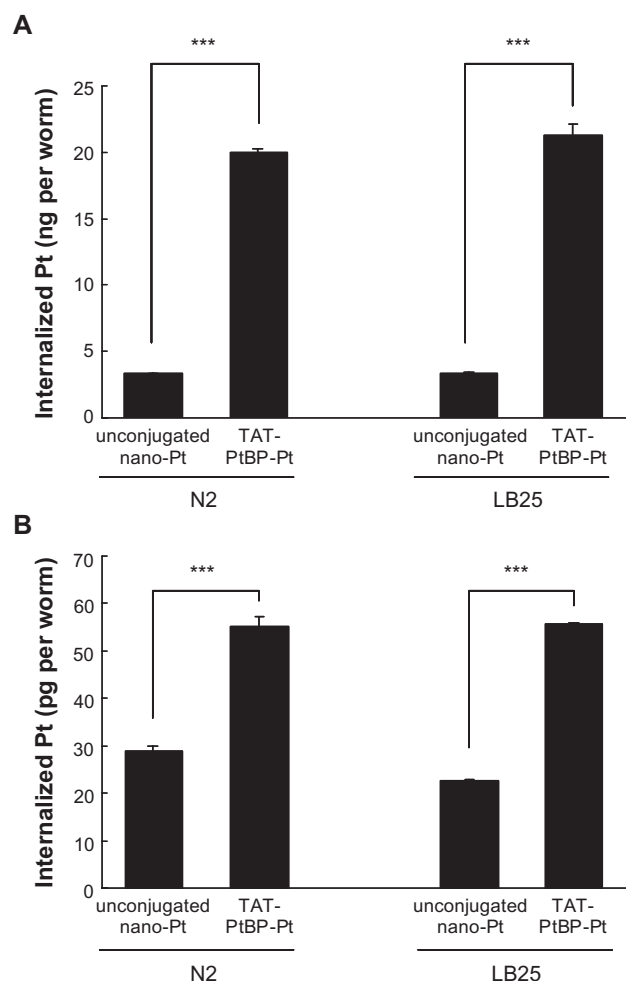


Figure 2 Amount of Pt internalized in whole bodies and mitochondria of N2 and LB25. Animals were treated with 5 μ M TAT-PtBP-Pt for five days from Day 0. Pt accumulation in worm whole bodies **A**) and mitochondria **B**) was determined by an inductively-coupled plasma mass spectrometer ICP-MS. For control, unjugated Pt-nps (PVP-Pt) was used. The number of worms used was 100 and 500–508 in each measurement for whole bodies and mitochondria, respectively, and three independent experiments were repeated. Error bars represent the standard error of the mean.

Note: Statistical significance was determined by Student's *t*-test (** $P < 0.001$).

from mitochondrial MitoSox was 48.0 ± 3.0 and 45.7 ± 2.8 in control N2 and LB25, respectively (Figure 4E depicted with relative fluorescence). A similar treatment with 5 μ M TAT-PtBP-Pt significantly decreased the MitoSox fluorescence (39.6 ± 2.7 ; $*P < 0.05$ and 35.9 ± 2.0 ; $**P < 0.01$ as intensity in N2 and LB25, respectively). These results show that ROS accumulation in control LB25 is not excessive, and TAT-PtBP-Pt treatment decreases ROS in N2 and LB25 to a similar extent. A main cause of the short life of LB25 may not be ROS accumulation.

We measured cytosolic and mitochondrial ROS in LB25 for the first time. Excessive accumulation of ROS was not observed in the cytosol or mitochondria of control LB25 in comparison with control N2. We think that the quantification of ROS level is insufficient due to the ROS estimation by

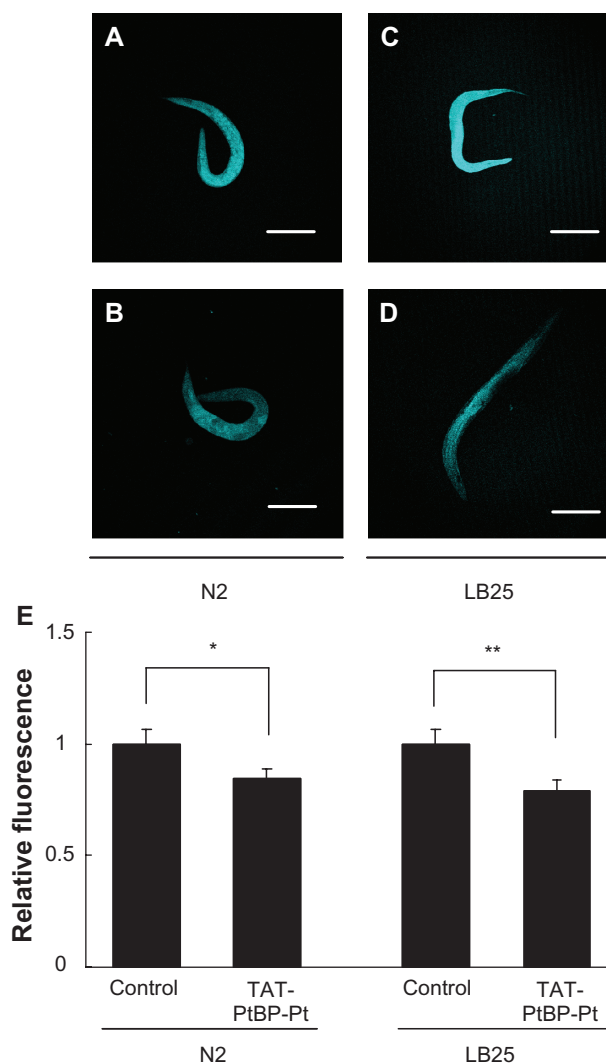


Figure 3 Effects of TAT-PtBP-Pt on cytosolic reactive oxygen species in N2 and LB25. Animals were treated with 5 μ M TAT-PtBP-Pt for five days from Day 0. Worms were then treated with 10 μ M CM-H₂DCFDA for 30 minutes at 20°C. Fluorescence was measured by confocal fluorescence microscopy (Ex 488 nm and Em 510 nm). Shown is cytosolic reactive oxygen species in N2 and LB-25 whole bodies: **A**) control N2; **B**) treated N2; **C**) control LB25; **D**) treated LB25. The panel **E**) shows the average of relative intensity for three independent experiments with 10 worms per each experiment. Error bars represent the standard error of the mean.

Notes: $*P < 0.05$; $**P < 0.01$, as compared with control worms by Student's *t*-test.

fluorescent dyes. However, these results are still interesting. It has been reported that 1-methyl-4-phenylpyridinium and rotenone, inhibitors of complex I, lead to NADH-dependent generation of O₂^{•−} using prepared bovine mitochondrial particles.³³ However, this increase of O₂^{•−} generation by the inhibitors was measured for a short period. Thus, we have to study the perturbation of ROS level by suppression of complex I for a long time *in vivo*. In fact, oxygen consumption was reduced by 50% in LB25, compared with N2.¹⁸ Decreased oxygen consumption is supposed to help decrease the generation of ROS. Currently, we do not know how LB25 worms maintain ROS at a relatively normal level during life. Because the

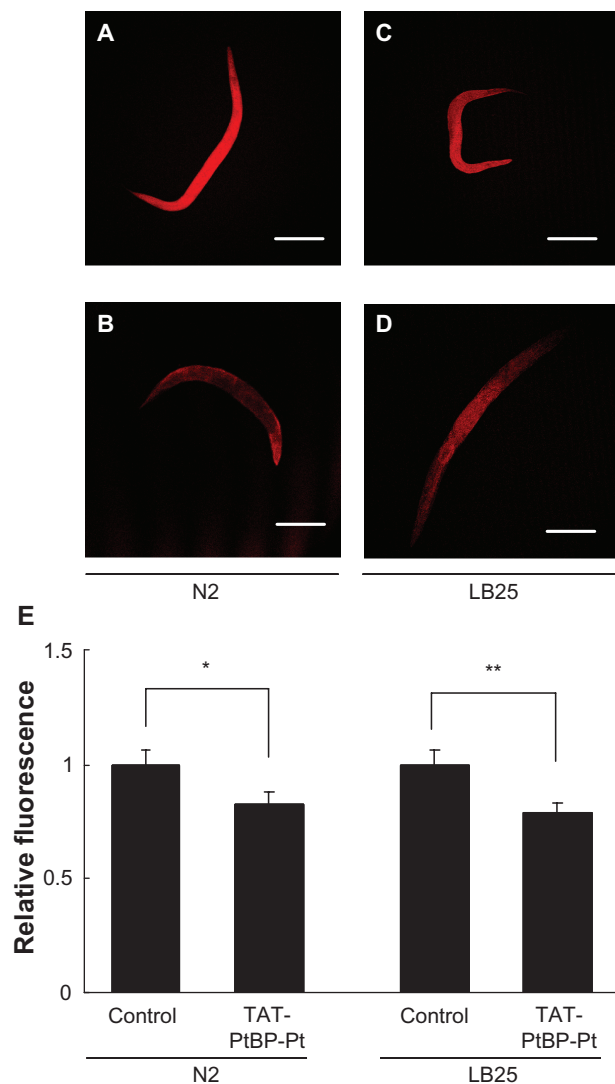


Figure 4 Effects of TAT-PtBP-Pt on O_2^- in N2 and LB25 mitochondria. Animals were cultured with TAT-PtBP-Pt for five days from Day 0. Worms were then treated with 10 μ M MitoSOX for 30 minutes at 20°C. Fluorescence was measured by confocal fluorescence microscopy (Ex 510 nm and Em 580 nm). Shown is O_2^- in N2 and LB25 mitochondria: **A)** control N2; **B)** treated N2; **C)** control LB25; **D)** treated LB25. The panel **E)** shows the average of relative intensity for three independent experiments with 10 worms per each experiment. Error bars represent the SEM. **Notes:** * $P < 0.05$; ** $P < 0.01$, as compared with control worms by Student's *t*-test.

oxidative state must be high in LB25, oxidized substances may be accumulated to reduce free ROS. Oxidative marker assays will be required.

Increase of $[NAD^+]/[NADH]$ ratio in *nuo-1* by TAT-PtBP-Pt

We measured NAD^+ and $NADH$ levels in the whole body homogenate and mitochondrial fraction from N2 and LB25. The $[NAD^+]/[NADH]$ ratio was considerably smaller in the whole body (0.057 ± 0.004) and mitochondria (0.026 ± 0.005) of control LB25 than in those of control N2 (whole body, 0.167 ± 0.005 ; mitochondria, 0.146 ± 0.006), indicating

excessive accumulation of $NADH$ in LB25 (Figure 5). Treatment of N2 with 5 μ M TAT-PtBP-Pt significantly increased the $[NAD^+]/[NADH]$ ratio by approximately twice (** $P < 0.001$). A similar treatment of LB25 with 5 μ M TAT-PtBP-Pt greatly increased the $[NAD^+]/[NADH]$ ratio by 4.6 and 8.8 times in whole body and mitochondria, respectively (** $P < 0.001$). These results indicate that Pt-nps function as $NADH$ oxidase in *C. elegans*, and accumulated $NADH$ in LB25 is efficiently oxidized to NAD^+ . This recovery of the $[NAD^+]/[NADH]$ ratio may take part in the effective lifespan extension of LB25.

In *nuo-1* mutants, including LB25, excessive cellular $NADH$ caused reduction of pyruvate to lactate.¹⁸ Depletion of pyruvate slows down tricarboxylic acid cycle and oxidative phosphorylation. We believe that Pt-nps oxidize $NADH$ to NAD^+ to normalize the $NAD^+/NADH$ ratio, which recovers

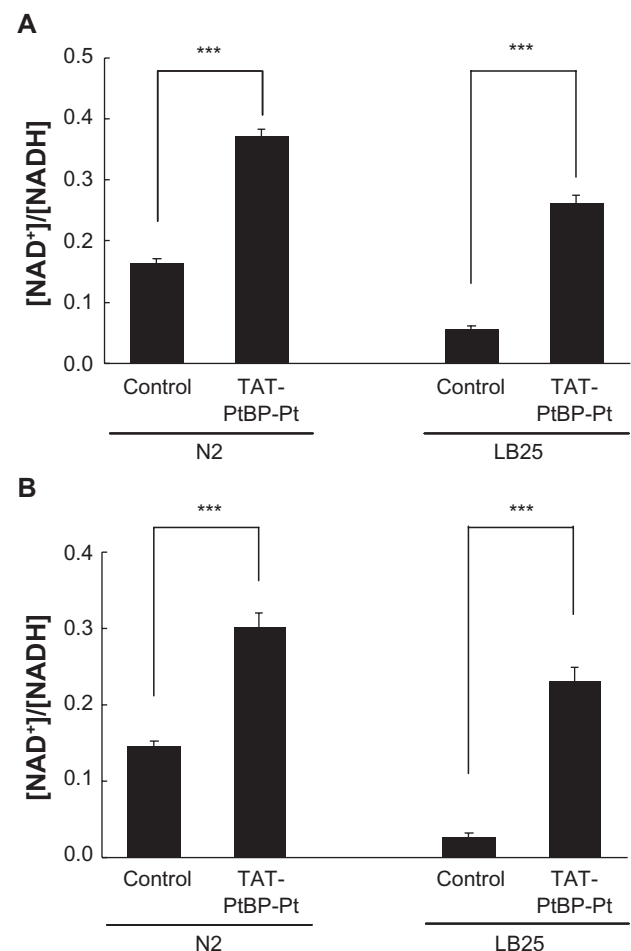


Figure 5 Effects of TAT-PtBP-Pt on the $[NAD^+]/[NADH]$ ratio in N2 and LB25. The concentrations of NAD^+ and $NADH$ were measured in whole bodies **A)** and mitochondria **B)** using an assay kit. The number of worms was 100 and 500 in each measurement for whole bodies and mitochondria, respectively, and three independent experiments were repeated. Error bars represent the standard error of the mean.

Note: *** $P < 0.001$ as compared with control worms by Student's *t*-test.

these metabolic pathways and increases adenosine triphosphate synthesis, even though the activity of complex IV is decreased by approximately 50%.¹⁸ Increase of adenosine triphosphate helps recover the short life of LB25. One may think that accelerated oxidative phosphorylation may produce O_2^- as a byproduct because LB25 has the low activity of complex I. Pt-nps are able to scavenge ROS including O_2^- . A similar decrease of ROS by TAT-PtBP-Pt treatment was observed in the cytosol and mitochondria of N2 and LB25 (Figures 3 and 4). However, if Pt-nps efficiently scavenge more ROS in treated LB25, a similar decrease of ROS may be apparent. The lifespan recovery of LB25 by Pt-nps may be supported by the maintenance of ROS using Pt-nps. We believe that the NADH oxidase activity of Pt-nps in scavenging ROS plays a pivotal role in effective recovery of the short lifespan of LB25.

Furthermore, even in wild-type N2, the $[NAD^+]/[NADH]$ ratio was increased by treatment with Pt-nps. The NAD^+ -dependent SIR-2.1 pathway may be involved in the lifespan extension caused by treatment with Pt-nps.³⁴ If it is, this signal pathway seems to be more effective in LB25 to elongate the lifespan because of a marked increase of NAD^+ by Pt-nps treatment.

Conclusion

Pt-nps functionalized with a TAT fusion protein are internalized in the mitochondria as well as in the cytosol and exert NADH oxidase activity. Therefore, Pt-np species may be a potent medicinal material to improve symptoms caused by mitochondrial complex I defect. Active targeting of the Pt-nps to mitochondrial matrix and/or inner membrane using signal peptides will be helpful to develop this potency further.

Acknowledgment

This work was supported in part by a Grant-in-Aid for Scientific Research from the Ministry of Education, Culture, Sports, Science, and Technology, Japan.

Disclosure

The authors report no conflicts of interest in this work.

References

- Kajita M, Hikosaka K, Iitsuka M, Kanayama A, Toshima N, Miyamoto Y. Platinum nanoparticle is a useful scavenger of superoxide anion and hydrogen peroxide. *Free Rad Res*. 2007;41:615–626.
- Cao Z, Zou Y, Xiang C, Sun LX, Xu F. Amperometric glucose biosensor based on ultrafine platinum nanoparticles. *Anal Lett*. 2007;40:2116–2127.
- Polsky R, Gill R, Kaganovsky L, Willner I. Nucleic acid-functionalized Pt nanoparticles: Catalytic labels for the amplified electrochemical detection of biomolecules. *Anal Chem*. 2006;78:2268–2271.
- Bhattacharya R, Mukherjee P. Biological properties of “naked” metal nanoparticles. *Adv Drug Deliv Rev*. 2008;60:1289–1306.
- Boisselier E, Astruc D. Gold nanoparticles in nanomedicine: Preparation, imaging, diagnostics, therapies and toxicity. *Chem Soc Rev*. 2009;38:1759–1782.
- Ghosh P, Han G, De M, Kim CK, Rotello VM. Gold nanoparticles in delivery applications. *Adv Drug Deliv Rev*. 2008;60:1307–1315.
- Barone M, Sciortino MT, Zaccaria D, Mazzaglia A, Sortino S. Nitric oxide photocaging platinum nanoparticles with anticancer potential. *J Mater Chem*. 2008;18:5531–5536.
- Zang L, Laug L, Münchgesang W, et al. Reducing stress on cells with apoferritin-encapsulated platinum nanoparticles. *Nano Lett*. 2010;19:219–223.
- Pelka J, Gehrke H, Esselen M, et al. Cellular uptake of platinum nanoparticles in human colon carcinoma cells and their impact on cellular redox systems and DNA integrity. *Chem Res Toxicol*. 2009;22:649–659.
- Watanabe A, Kajita M, Kim J, et al. In vitro free radical scavenging activity of platinum nanoparticles. *Nanotechnology*. 2009;20:455105.
- Kim J, Takahashi M, Shimizu T, et al. Effects of a potent antioxidant, platinum nanoparticle, on the lifespan of *Caenorhabditis elegans*. *Mech Ageing Dev*. 2008;129:322–331.
- Hirst J. Towards the molecular mechanism of respiratory complex I. *Biochem J*. 2010;425:327–339.
- Schuelke M, Smeitink J, Mariman E, et al. Mutant *NDUFV1* subunit of mitochondrial complex I causes leukodystrophy and myoclonic epilepsy. *Nat Genet*. 1999;21:260–261.
- Bénit P, Chretien D, Kadhon N, et al. Large-scale deletion and point mutations of nuclear *NDUFV1* and *NOUFS1* genes in mitochondrial complex I deficiency. *Am J Hum Genet*. 2001;68:1344–1352.
- Winklhofer K, Haass C. Mitochondrial dysfunction in Parkinson's disease. *Biochim Biophys Acta*. 2010;1802:29–44.
- Korenaga M, Okuda M, Otani K, Wang T, Li Y, Weinman SA. Mitochondrial dysfunction in hepatitis C. *J Clin Gastroenterol*. 2005;39:s162–s166.
- Hikosaka K, Kim J, Kajita M, Kanayama A, Miyamoto Y. Platinum nanoparticles have an activity similar to mitochondrial NADH: Ubiquinone oxidoreductase. *Colloids Surf Biointerfaces*. 2008;66:195–200.
- Grad LI, Lemire BD. Mitochondrial complex I mutations in *Caenorhabditis elegans* produce cytochrome c oxidase deficiency, oxidative stress and vitamin-responsive lactic acidosis. *Hum Mol Genet*. 2004;13:303–314.
- Brenner S. The genetics of *Caenorhabditis elegans*. *Genetics*. 1974;77:71–94.
- Sulston JE, Brenner S. The DNA of *Caenorhabditis elegans*. *Genetics*. 1974;77:95–104.
- Järver P, Langel Ü. Cell-penetrating peptides – A brief introduction. *Biochim Biophys Acta*. 2006;1758:260–263.
- Sarikaya M, Tamerler C, Jen AKY, Schulten K, Baneyx F. Molecular biomimetics: Nanotechnology through biology. *Nat Mater*. 2003;2:577–585.
- Kim J, Shirasawa T, Miyamoto Y. The effect of TAT conjugated platinum nanoparticles on lifespan in a nematode *Caenorhabditis elegans* model. *Biomaterials*. 2010;31:5849–5854.
- Johnson TE, Wood WB. Genetic analysis of the life-span of *Caenorhabditis elegans*. *Proc Natl Acad Sci U S A*. 1982;79:6603–6607.
- Heidler T, Harwing K, Daniel H, Wenzel U. *Caenorhabditis elegans* lifespan extension caused by treatment with an orally active ROS-generator in dependent on DAF-16 and SIR-2.1. *Biogerontology*. 2010;11:183–195.
- El-Andaloussi S, Holm T, Langel Ü. Cell-penetrating peptides: Mechanisms and Applications. *Curr Pharm Des*. 2005;11:3597–3611.
- Vivès E, Lebleu B. The tat-derived cell-penetrating peptide. In: Langel Ü, editor. *Cell-Penetrating Peptides: Processes and Applications*. Boca Raton, FL: CRC Press LLC; 2002.
- Delom F, Fessart D, Caruso ME, Chevet E. Tat-mediated protein delivery in living *Caenorhabditis elegans*. *Biochem Biophys Res Commun*. 2007;352:587–591.

29. Wagstaff KM, Jans DA. Protein transduction: Cell penetrating peptides and their therapeutic applications. *Curr Med Chem*. 2006;13: 1371–1387.
30. de la Fuente JM, Berry CC. Tat peptide as an efficient molecule to translocate gold nanoparticles into the cell nucleus. *Bioconjug Chem*. 2005;16:1176–1180.
31. Berry CC, de la Fuente JM, Mullin M, Chu SWI, Curtis ASG. Nuclear localization of HIV-1 tat functionalized gold nanoparticles. *IEEE Trans Nanobiosci*. 2007;6:262–269.
32. Ross MF, Murphy MP. Cell-penetrating peptides are excluded from the mitochondrial matrix. *Biochem Soc Trans*. 2004;32:1072–1074.
33. Hasegawa E, Takeshige K, Oishi T, Murai Y, Minakami S. 1-Methyl-4-phenylpyridinium (MPP⁺) induces NADH-dependent superoxide formation and enhances NADH-dependent lipid peroxidation in bovine heart submitochondrial particles. *Biochem Biophys Res Commun*. 1990;170:1049–1055.
34. Tissenbaum H, Gurente L. Increased dosage of a *sir-2* gene extends lifespan in *Caenorhabditis elegans*. *Nature*. 2001;410:227–230.

International Journal of Nanomedicine

Publish your work in this journal

The International Journal of Nanomedicine is an international, peer-reviewed journal focusing on the application of nanotechnology in diagnostics, therapeutics, and drug delivery systems throughout the biomedical field. This journal is indexed on PubMed Central, MedLine, CAS, SciSearch®, Current Contents®/Clinical Medicine,

Submit your manuscript here: <http://www.dovepress.com/international-journal-of-nanomedicine-journal>

Journal Citation Reports/Science Edition, EMBase, Scopus and the Elsevier Bibliographic databases. The manuscript management system is completely online and includes a very quick and fair peer-review system, which is all easy to use. Visit <http://www.dovepress.com/testimonials.php> to read real quotes from published authors.

Dovepress